engineering proceedings

MDPI

Proceeding Paper

In Silico Analysis of Toehold-Aptamer Sequences Targeting the SARS-CoV-2 Nucleocapsid Protein Gene for Biosensor Development †

Karla M. Esquivel-Ortiz *, Aurora Antonio-Pérez and Ana L. Torres-Huerta

Department of Engineering and Sciences, Monterrey Institute of Technology and Higher Education, Av. Lago de Guadalupe KM 3.5, Margarita Maza de Juarez, Ciudad Lopez Mateos 52926, Mexico
* Correspondence: a01366240@tec.mx
† Presented at the 3rd International Electronic Conference on Biosensors, 8–21 May 2023; Available online: https://iecb2023.sciforum.net/.

Abstract: The COVID-19 pandemic has emphasized the need for rapid and affordable on-site virus detection. While enzyme-linked aptamer-based biosensors have proven effective, their utility for SARS-CoV-2 detection remains unexplored. We performed in silico analysis of three toehold-aptamer sequences targeting the SARS-CoV-2 nucleocapsid protein gene, with secondary and tertiary structures modeled using mFold and RNAComposer web servers. Molecular docking simulations were challenging due to computational and molecular constraints. Nevertheless, our findings indicate that experimental procedures to assess aptamer–target interactions in vitro under optimal assay conditions are feasible. Successful development of a biosensor using these aptamers could offer a quick and inexpensive method for SARS-CoV-2 detection, addressing the COVID-19 pandemic.

Keywords: SARS-CoV-2 virus; biosensors; aptamers; nanozymes; point-of-care-diagnosis; COVID-19 disease; toehold technology; computational assays

check for updates

Citation: Esquivel-Ortiz, K.M.; Antonio-Pérez, A.; Torres-Huerta, A.L. In Silico Analysis of Toehold-Aptamer Sequences Targeting the SARS-CoV-2 Nucleocapsid Protein Gene for Biosensor Development. *Eng. Proc.* **2023**, *35*, 21. https://doi.org/10.3390/IECB2023-14718

Academic Editor: Sara Tombelli

Published: 23 May 2023

Copyright: © 2023 by the authors. Licensee MDPI, Basel, Switzerland. This article is an open access article distributed under the terms and conditions of the Creative Commons Attribution (CC BY) license (https://creativecommons.org/licenses/by/4.0/).

1. Introduction

The severe acute respiratory syndrome coronavirus 2 (SARS-CoV-2) is a single-stranded positive-sense RNA (+ss-RNA) virus with a ~29.9 kb linear genome that belongs to the viral family Coronaviridae. SARS-CoV-2 emerged in Wuhan, China, at the end of 2019 as a new deadly coronavirus known as COVID-19 [1–3]. Mexico is among the countries that have been severely affected by the disease, mainly due to the underlying population risk factors, such as cardiovascular diseases, including dyslipidemia, hypertension, and type 2 diabetes. These factors have resulted in a syndemic situation in which poverty and limiting social factors, such as access to health care, are determinants of the epidemiological outcome [4].

The SARS-CoV-2 viral genome consists of two major open reading frames (ORFs), ORF1a and ORF1b, that encode 16 non-structural proteins of which most compose the viral replication and transcription complex [5]. The remaining one-third of the genome at the 3′-end has overlapping ORFs that encode four major structural proteins, spike glycoprotein (S), membrane (M), envelope (E), and nucleocapsid (N) proteins [3]. Along with a lipid bilayer derived from the host, these structural proteins form an enveloped virion, or virus particle, that delivers viral genomic RNA into the cell. Mutations in the viral genome have led to the establishment of genetic groups called lineages, which differ from one another, resulting in the emergence of variants [6], including those categorized as variants of concern (VOCs) by the World Health Organization (WHO) [7]. In Mexico several variants have been detected, including the Alpha, Beta, Gamma, Delta, and Omicron VOCs. Other high-frequency variants more prevalent in Mexico than in the rest of the world include lineages B.1.1.222 (10.3% presence) and descendant B.1.1.519 (37.8% presence), the latter being the dominant virus in Mexico from 2020 until now [4]. Several diagnostic methods are available

for detecting SARS-CoV-2. However, these methods have several limitations, including lower accuracy and sensitivity; troublesome sampling preparation and purification; time-consuming procedures; special equipment, accessories, and maintenance cost; limited large-scale availability; complex instrument operation; the requirement for highly qualified technical personnel; and unsuitability for rapid on-site analysis [8,9]. Consequently, there is a need to develop newer, more efficient methods for rapidly detecting viral analytes, considering the versatility of viruses and their replication niches. Implementing these methods must ensure higher accuracy, ease of operation and portability, and large-scale availability to test the mass population [10,11].

Biosensing technology, specifically DNA/RNA aptasensors, has recently emerged as a promising method for detecting SARS-CoV-2, due to their high-affinity and specificity for target recognition [12,13]. Aptamers, single-stranded oligonucleotides, can be utilized to target different SARS-CoV-2 proteins, including the nucleocapsid (N), which has been suggested as a potential biomarker for early diagnosis due to its abundant expression and low genetic variation over time (Appendix A Figure A1) [14]. Computational methods have become increasingly popular for aptamer screening and interaction studies, including in silico modeling of aptamer structures and molecular docking simulations [15].

This project aims to develop a lab-on-a-chip optical aptasensor for detecting SARS-CoV-2 in saliva using a toehold-aptamer strategy for signal amplification. As a first step, this study analyzed in silico three proposed toehold-aptamer sequences targeting the SARS-CoV-2 nucleocapsid protein gene (Gene ID: 43740575). Tools like mFold and RNAComposer were employed to model the aptamers' secondary and tertiary structures. On the other hand, we attempted to establish molecular docking simulations; however, simulations were challenging to produce due to limitations in computational hardware and the large number of atoms inherent in DNA molecules. Efforts to perform docking simulations will continue. Nevertheless, based on the current findings, experimental procedures will be conducted using optimal assay conditions to assess aptamer-target interactions in vitro.

2. Computational Methods

2.1. Structure Retrieval

The toehold-aptamer sequences (v1, v2, v3), 23–24 nt length (Appendix A Table A1**)**, are in the 28,000–29,000 region of the SARS-CoV-2 genome, where the 'N' gene (Gene ID: 43740575) translated into Nucleocapsid Phosphoprotein (N)- The 'N' gene was chosen as the target molecule due to its high conservation among coronaviruses and greater stability and lower mutation rates compared to the 'S' protein.

2.2. Multiple Sequence Alignment Analysis

Two Multiple Sequence Alignment (MSA) analyses were assessed. (1) SARS-CoV-2 'N' gene conservation among other coronaviruses using NCBI GenBank database to obtain genome sequences of various CoV isolates from humans, bats, civets, and pangolins, analyzed via BLAST against the Wuhan-Hu-1/2019 reference genome, with percent sequence identity. (2) Aptamer sequence conservation among Mexican COVID-19 variants using NCBI Virus online platform and MEGA X software.

2.3. Aptamers' 2D-Structure Prediction

The mFold online server (http://www.unafold.org/ (accessed on 8 April 2023)) generated secondary structures based on parameters such as folding temperature and sodium (Na^+) and magnesium (Mg^{2+}) ionic concentrations. We tested temperatures (4, 27, 37 °C), sodium concentrations (0, 25, 50, 75, 100 mM), and magnesium concentrations (5, 10, 15, 20 mM). After analyzing all combinations, we chose the 2D-structures with the lowest free energy for further study.

2.4. Aptamers' 3D Modeling

Using dot-bracket notation for 2D topology, the RNA Composer online server ("https://rnacomposer.cs.put.poznan.pl/" (accessed on 8 April 2023)) created the aptamers' tertiary (3D) structures. Given that RNAComposer exclusively processes RNA sequences, the original sequences underwent modification by replacing 'T' with 'U'. AVOGADRO software was employed to minimize the generated 3D-structures, and 3DNA web server ("http://web.x3dna.org/mutation_file/mutationsel" (accessed on 8 April 2023)) was used to transform RNA to DNA structures. The resultant .pdb files were imported into PyMOL software for 3D modeling.

2.5. Molecular Docking

In the docking simulation, the positive control sequence (C+) interacted with aptamers. The (C+) and optimized 3D toehold-aptamer structures were imported into Chimera, assigned as 'ligand' and 'receptor.' Surface binding analysis using AutoDock Vina was the preferred method. Simultaneously, efforts were made to conduct docking simulations using PyRx and AutoDock software.

3. Results and Discussion

3.1. Multiple Sequence Alignment Results

Based on the results of the two multiple alignments conducted, it was determined that the SARS-CoV-2 genomes are highly conserved among coronaviruses. Moreover, the proposed aptameric sequences were also found to be highly conserved among 193 variants of SARS-CoV-2.

To identify conserved and potentially functional features within the CoV family, this study compared the 'N' gene of SARS-CoV-2 against selected CoV families. The analysis revealed an identity ranging from 87% to 96% with isolates from the reference Wuhan H-1 sequences. Thus, the SARS-CoV-2 N gene exhibited significant sequence conservation with other CoV families, suggesting it holds significant potential as a biomarker for early diagnosis [14]. These findings align with prior research concerning the genetic similarity and conservation of key proteins among SARS-CoV-2 and other coronaviruses. Consequently, these features could be exploited for the development of the biosensing tool technology pursued in this project. The use of conserved regions as diagnostic targets could significantly enhance the accuracy and speed of testing.

Furthermore, the multiple sequence alignment (MSA) of the aptameric sequences showed that trigger sequences *v1* and *v2* were highly conserved across all COVID-19 variants, while trigger v3 displayed a slight variation in position 28806 with a 'T' instead of a 'C' in two out of 193 analyzed sequences (ON482441.1(+) and ON482444.1(+)). Nevertheless, these results imply that the proposed sequences can be utilized to identify different SARS-CoV-2 variants present in Mexico. The findings regarding the conserved aptameric sequences present potential diagnostic applications for identifying different SARS-CoV-2 variants in Mexico.

3.2. Aptamers' 2D Structure and Free Energy

As previously mentioned, the mFold algorithm can generate multiple predictions based on various running parameters, such as folding temperature and ionic concentration of Na^+ and Mg^{2+}. The assay conditions we examined were based on previous studies that proposed aptamers as bioreceptor elements for targeting SARS-CoV-2 proteins or genomic material. Along with the stability analysis of the aptamers, we also investigated the stability of the positive control (C+) and negative control sequences (C−), which we plan to use in subsequent experiments, as well as the SARS-CoV-2 previously developed aptamers. The results obtained are displayed in Figure 1.

ID	[Mg++] mM	[Na+] mM																	
		0	1	25	50	75	100	0	1	25	50	75	100	0	1	25	50	75	100
		4 °C						25 °C						37 °C					
V1	0	1.06	-0.9	-1.56	-1.7	-1.78	-1.84	1.74	0.45	-0.7	-0.19	-0.25	-0.32	2.15	1.23	0.68	0.56	0.5	0.44
	5	-2.02	-2.02	-2.04	-2.06	-2.08	-2.08	-0.5	-0.5	-0.52	-0.54	-0.56	-0.58	0.3	0.3	0.28	0.26	0.25	0.24
	10	-2.08	-2.08	-2.1	-2.12	-2.12	-2.14	-0.58	-0.58	-0.59	-0.6	-0.62	-0.64	0.24	0.24	0.23	0.22	0.2	0.2
	15	-2.12	-2.12	-2.14	-2.16	-2.16	-2.17	-0.62	-0.62	-0.64	-0.64	-0.66	-0.67	0.2	0.2	0.2	0.18	0.17	0.17
	20	-2.16	-2.16	-2.16	-2.18	-2.19	-2.2	-0.64	-0.65	-0.66	-0.68	-0.68	-0.69	0.18	0.18	0.17	0.17	0.14	0.12
V2	0	-1.12	-1.05	-1.7	-1.85	-1.93	-1.98	-0.08	0.81	0.11	-0.04	-0.13	-0.2	0.5	1.82	1.14	0.98	0.9	0.82
	5	-2.17	-2.17	-2.18	-2.21	-2.21	-2.22	-0.38	-0.38	-0.4	-0.42	-0.44	-0.46	0.63	0.63	0.61	0.58	0.57	0.55
	10	-2.22	-2.22	-2.25	-2.26	-2.26	-2.29	-0.46	-0.46	-0.47	-0.49	-0.5	-0.52	0.55	0.55	0.54	0.53	0.5	0.5
	15	-2.26	-2.26	-2.29	-2.29	-2.3	-2.31	-0.5	-0.5	-0.52	-0.53	-0.54	-0.55	0.5	0.5	0.5	0.47	0.46	0.46
	20	-2.3	-2.3	-2.3	-2.33	-2.33	-2.34	-0.53	-0.53	-0.54	-0.56	-0.57	-0.58	0.47	0.47	0.46	0.46	0.43	0.42
V3	0	0.02	-3.35	-4.33	-4.55	-4.67	-4.75	1.15	-1.07	-2.11	-2.34	-2.47	-2.57	1.8	0.25	-0.85	-1.09	-1.21	-1.33
	5	-5.01	-5.01	-5.05	-5.07	-5.1	-5.12	-2.85	-2.85	-2.88	-2.91	-2.94	-2.97	-1.61	-1.61	-1.65	-1.69	-1.71	-1.73
	10	-5.11	-5.11	-5.15	-5.17	-5.17	-5.21	-2.96	-2.96	-2.99	-3.01	-3.03	-3.05	-1.73	-1.73	-1.75	-1.77	-1.81	-1.81
	15	-5.17	-5.17	-5.21	-5.22	-5.23	-5.24	-3.03	-3.03	-3.05	-3.07	-3.09	-3.11	-1.81	-1.81	-1.81	-1.85	-1.87	-1.87
	20	-5.23	-5.23	-5.23	-5.25	-5.27	-5.29	-3.07	-3.07	-3.09	-3.11	-3.13	-3.14	-1.85	-1.85	-1.87	-1.87	-1.91	-1.93
V1d	0	-0.53	-4.67	-6.3	-6.66	-6.87	-7.01	0.41	-1.57	-3.31	-3.7	-3.91	-4.09	0.7	0.02	-1.63	-2.03	-2.23	-2.46
	5	-7.44	-7.44	-7.5	-7.54	-7.59	-7.61	-4.6	-4.6	-4.66	-4.72	-4.78	-4.84	-3.01	-3.01	-3.11	-3.18	-3.23	-3.25
	10	-7.61	-7.61	-7.66	-7.7	-7.71	-7.76	-4.84	-4.84	-4.87	-4.91	-4.96	-5.01	-3.25	-3.25	-3.3	-3.35	-3.42	-3.42
	15	-7.71	-7.71	-7.76	-7.79	-7.81	-7.83	-4.96	-4.96	-5.01	-5.03	-5.08	-5.1	-3.42	-3.42	-3.42	-3.49	-3.54	-3.54
	20	-7.8	-7.8	-7.81	-7.84	-7.87	-7.9	-5.04	-5.06	-5.08	-5.13	-5.15	-5.19	-3.49	-3.49	-3.54	-3.54	-3.61	-3.66
C(+)	0	-1.91	-2.06	-3.2	-3.45	-3.61	-3.85	-0.43	0	-1	-1.26	-1.42	-1.52	0.25	1.16	0.24	-0.02	-0.16	-0.3
	5	-4.54	-4.54	-4.63	-4.7	-4.75	-4.82	-1.85	-1.85	-1.89	-1.92	-1.96	-1.99	-0.62	-0.62	-0.68	-0.72	-0.75	-0.76
	10	-4.81	-4.82	-4.88	-4.95	-4.98	-5.04	-1.99	-1.99	-2.01	-2.05	-2.06	-2.08	-0.76	-0.76	-0.79	-0.82	-0.86	-0.86
	15	-4.98	-4.98	-5.03	-5.07	-5.13	-5.14	-2.06	-2.06	-2.08	-2.12	-2.13	-2.15	-0.86	-0.86	-0.86	-0.9	-0.93	-0.93
	20	-5.11	-5.11	-5.14	-5.18	-5.22	-5.27	-2.12	-2.12	-2.13	-2.15	-2.19	-2.19	-0.9	-0.9	-0.93	-0.93	-0.97	-1
C(-)	0	1.17	-2.59	-3.56	-3.78	-3.91	-3.99	1.81	-0.59	-1.63	-1.86	-1.99	-2.1	2.2	0.57	-0.53	-0.77	-0.89	-1.01
	5	-4.24	-4.24	-4.28	-4.3	-4.34	-4.35	-2.37	-2.37	-2.4	-2.43	-2.46	-2.49	-1.29	-1.29	-1.33	-1.37	-1.39	-1.41
	10	-4.35	-4.35	-4.38	-4.4	-4.41	-4.44	-2.49	-2.49	-2.51	-2.53	-2.55	-2.58	-1.41	-1.41	-1.43	-1.47	-1.49	-1.49
	15	-4.41	-4.41	-4.44	-4.46	-4.47	-4.48	-2.55	-2.55	-2.58	-2.59	-2.61	-2.63	-1.49	-1.49	-1.49	-1.53	-1.55	-1.55
	20	-4.46	-4.46	-4.47	-4.48	-4.51	-4.52	-2.59	-2.6	-2.61	-2.64	-2.65	-2.67	-1.53	-1.53	-1.55	-1.55	-1.59	-1.61

Figure 1. Free energy of toehold-aptamers and control sequences at different assay conditions. The 3D modeling of aptamer sequences was predicted by RNAComposer online server, and free energy was obtained in the 2D structure analysis by mFold online server. Green cells represent great stability and functionality of the aptamers (free energy < −1.99 kcal/mol), yellow cells represent medium stability of the aptamers (−1.99 < free energy < 0 kcal/mol), while red cells indicate non-stable and non-functional structures (0 kcal/mol < free energy).

Our analysis of experimentally selected aptamers revealed a significant correlation between free energy structure formation and the running parameters of assay conditions. We found that the free energy of aptamers is significantly lower at magnesium (Mg^{2+}) concentrations of 20 mM and sodium (Na^{+}) concentrations of 100 mM. It was observed that although Na^{+} ions are essential, the variation in Mg^{2+} concentrations played a pivotal role in maintaining the stability of the aptamers. These findings align with previous studies, which utilized Na^{+} concentrations greater than 75 mM and Mg^{2+} concentrations above 10 mM to identify the best candidate aptamer sequences. Another noteworthy observation from this study is that as the assay's running temperature increased, the aptamers' structures began to lose stability and reached maximum free energy values at 37 °C, with the lowest free energy values occurring at 4°C. This observation is consistent with the literature, which suggests that shorter aptamer sequences are more unstable at higher temperatures due to their small size and susceptibility to temperature-induced disturbances.

From these studies, we determined that the optimal structures for all examined sequences were found at 4 °C, 20 mM Mg^{2+}, and 100 mM Na^{+}, where the structures exhibited the lowest free energy and highest stability. It is also important to note that among the three aptamers studied, the v3 aptamer demonstrated the highest stability and most closely aligned free energy values compared to those reported in the literature. Consequently, the

structures selected for 3D modeling were those discovered under the aforementioned assay conditions.

3.3. Aptamers' 3D Modeling

For aptamer sequences meeting our selection criteria, we generated their 3D structures. A detailed analysis of the experimental 3D structures for selected aptamers, offered a valuable insight into their molecular structure and any potential alterations that may occur when adjusting running parameters. The top three structures were then converted into .pdb format, and visualized using PyMOL software, as shown in Figure 2.

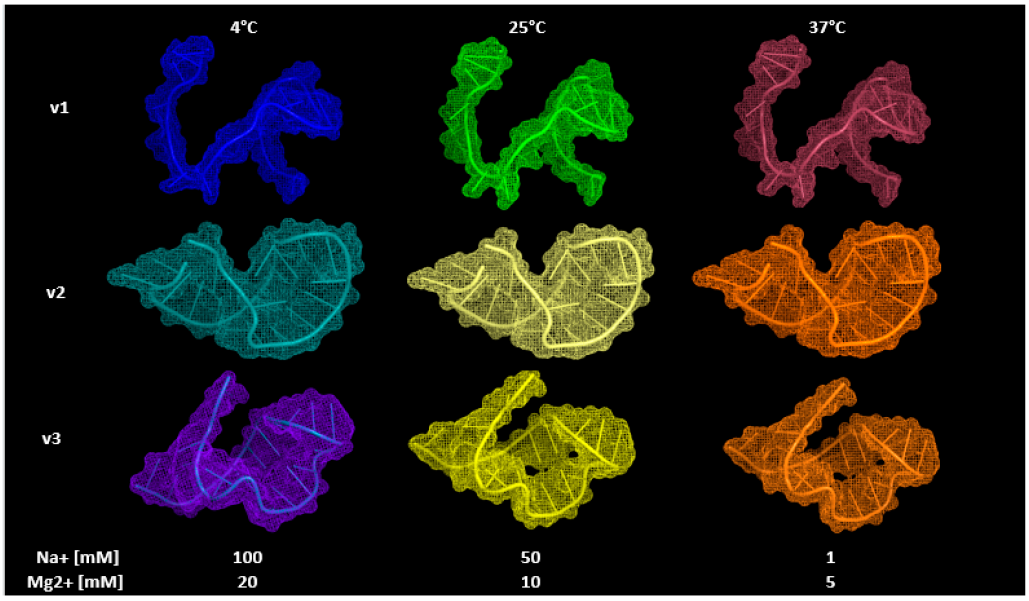


Figure 2. The 3D structures of most stable toehold-aptamer sequences at optimum assay conditions: optimum conditions are found at 4 °C, 100 mM Na^{+}, and 20 mM Mg^{2+}.

Additionally, we modeled the aptamers' 3D structures at varying running parameters to examine any changes within their structure (Figure 2). Our findings revealed that the aptamers' 3D structures remained unaffected despite alterations in the running parameters. This observation can be primarily attributed to the sequence length of the aptamers.

3.4. Molecular Docking

Computational docking is a widely used tool to identify small-molecule ligands binding to proteins. Various docking simulators were tried, including CHIMERA, AUTODOCK TOOLS, and PyRX, but proved infeasible, mainly due to the receptor's large atom count. These methods were primarily designed for proteins, and though AUTODOCK and DOCK can dock compounds to RNA/DNA molecules, both the ligand and receptor were DNA-based. Modeling DNA aptamers with DNA targets is complex due to their intricate nature. Existing docking software typically displays ligands bound to short DNA sequences and is tailored more for protein structures than DNA properties. Nevertheless, for experimental purposes, we opted to conduct further experimental procedures using the high-affinity aptamers identified in previous analyses, speeding up the desired interactions between the aptamers and the target sequence.

4. Conclusions

Our MSA analysis revealed that the conserved 'N' gene of SARS-CoV-2 could be used as a target molecule that can be used to develop the biosensing tool that this project aims for. Furthermore, our findings on the conserved aptameric sequences suggest they are potential bioreceptors to identify various SARS-CoV-2 variants in Mexico. In this study, we employed a computational approach to find the potential running parameters in which the

proposed DNA aptamers can find their highest stability and possible capacity of binding affinity to the desired target ligand. In the first level, we analyzed the secondary structure of the proposed sequences using varying parameters. For the sequences meeting our selection criteria, we generated their 3D structures. In the second level, we attempted computational docking to identify target–aptamer interactions. In the second screening, we attempted computational docking to identify target–aptamer interactions. However, due to the large number of atoms in the ligand and receptor molecules, this was not possible. Docking analysis will be attempted using other docking software to complete the screening of the proposed aptamers. Nonetheless, for experimental and project purposes, it has been decided that the high-affinity aptamers identified in this in silico analysis can be selected for carrying out experimental procedures, thus accelerating the understanding of the desired interactions between the aptamers and the target sequence.

Author Contributions: Conceptualization, K.M.E.-O., A.A.-P. and A.L.T.-H.; methodology, K.M.E.-O.; software, K.M.E.-O.; validation, K.M.E.-O.; formal analysis, K.M.E.-O.; investigation, K.M.E.-O., A.A.-P. and A.L.T.-H.; resources, K.M.E.-O.; data curation, K.M.E.-O.; writing—original draft preparation, K.M.E.-O.; writing—review and editing, K.M.E.-O.; visualization, K.M.E.-O.; supervision, A.A.-P. and A.L.T.-H.; project administration, K.M.E.-O., A.A.-P. and A.L.T.-H. All authors have read and agreed to the published version of the manuscript.

Funding: This research received no external funding.

Institutional Review Board Statement: Not applicable.

Informed Consent Statement: Not applicable.

Data Availability Statement: Not applicable.

Conflicts of Interest: The authors declare no conflict of interest.

Appendix A

Type	Aptamer Name	Sequence (5′–3′)	Target
ssDNA	A48	GCTGGATGTCGCTTACGACAATATTCCTTAGGGGCAC CGCTACATTGACACATCCAGC	SARS-CoV-2 N protein (Zhang_2020a)
	A58	GCTGGATGTCACCGGATTGTCGGACATCGGATTGTCT GAGTCATATGACACATCCAGC	
	A61	GCTGGATGTTGACCTTTACAGATCGGATTCTGTGGGG CGTTAAACTGACACATCCAGC	
	A15	GCTGGATGTTCATGCTGGCAAAATTCCTTAGGGGCAC CGTTACTTTGACACATCCAGC	
ssRNA	RNA-001	GGAAACGGAAUGUCGAUUUCGUGGUUAUCC	NSP10/NSP16 interface complex (Kothandan,2021)
	RNA-010	UUUGGCCAACGGGAGAGUUAAGGUCAUAAA	
ssDNA	tNSP1	TAACCACGGCGCAAGCCGGGGTGTACGTGTTATACGTGCGTGTATCGAG	SARS-CoV-2 N protein (Poolsup, 2023)
	tNSP2	CTGACTGTAACCACGTATTGCGTTCCAGTCCCTATGACCAACGTCACAATAAGTCGCATAGGTA	
	tNSP3	CAGCGTCACGTGTTGTTCCCCATTGTACTGATTCGTCGTGGCAT	
ssDNA	N Aptamer 1	bio-GCAATGGTACGGTACTTCCGGATGCGGAAACTGGCTAATTGGTGAGGCTGGGGCGGTCGTGCAGCAAAAGTGCACGCTACTTTGCTAA	SARS-CoV-2 N protein (Chen, 2020)
	N Aptamer 2	bio-GCAATGGTACGGTACTTCCGGATGCGGAAACTGGCTAATTGGTGAGGCTGGGGCGGTCGTGCAGCAAAAGTGCACGCT	
	N Aptamer 3	bio-GCAATGGTACGGTACTTCCGGATGCGGAAACTGGCTAATTGGTGAGGCTGGGGCGGT	
	Aptamer n.c.	bio- GCAATGGTACGGTACTTCCGGATGCGGAAACTG	
ssDNA	Apt 58	biotin-GCT GGA TGT CAC CGG ATT GTC GGA CAT CGG ATT GTC TGA GTC ATA TGA CAC ATC CAG C	SARS-CoV-2 N protein (Ge, 2022)
	Apt 61	biotin-GCT GGA TGT TGA CCT TTA CAG ATC GGA TTC TGT GGG GCG TTA AAC TGA CAC ATC CAG C	
L-DNA	C1t	TTGTGAGCCTCCTAACTAGGGGGTGGTGTGGGGGATTTGCGGGTCG GCTAGAGGCTCTCTGA	SARS-CoV-2 stem-loop II-like motif (s2m) RNA structure (Li, 2021)
	C3t	CAAGAAAAGCATCTAGGGGGTGGATGTGGGGGTTTAGAGGGCGTACATGCTTATTCTTGT	
ssDNA	N-48 aptamer	GCTGGATGTCGCTTACGACAATATTCCTTAGGGGCACCGCTACATTGACACATCCAGC	SARS-CoV-2 N protein (Zhou, 2022)

Figure A1. Developed aptamers targeting SARS-CoV-2 [15–21].

Table A1. Working Sequences: Toehold-Aptamer Sequences Targeting SARS-CoV-2 'N' Gene, Positive Control (C+), and Negative Control Sequences.

ID	Trigger	Length	Location
v1	5′- TCTTGGTTCACCGCTCTCACTCAA -3′	24	28,424–28,447
v2	5′- CGCTCTCACTCAACATGGCAAGG -3′	23	28,435–28,457
v3	5′- CTACGCAGAAGGGAGCAGAGGCGG -3′	24	28,786–28,809
C(+)	3′- GCAAATCTAGGCTTGCTGTTTGGG -5′	24	
C(−)	3′- TGCAGAAAAAAACCATGGGTTGGG -5′	24	

References

1. Wandtke, T.; Wędrowska, E.; Szczur, M.; Przybylski, G.; Libura, M.; Kopiński, P. Aptamers—Diagnostic and Therapeutic Solution in SARS-CoV-2. *Int. J. Mol. Sci.* **2022**, *23*, 1412. [CrossRef] [PubMed]
2. Santosh, T.S.; Parmar, R.; Anand, H.; Srikanth, K.; Saritha, M. A review of salivary diagnostics and its potential implication in detection of COVID-19. *Cureus* **2020**, *12*, e7708. [CrossRef] [PubMed]
3. Wu, X.; Chen, Q.; Li, J.; Liu, Z. Diagnostic techniques for COVID-19: A mini-review. *J. Virol. Methods* **2022**, *301*, 114437. [CrossRef] [PubMed]
4. García-López, R.; Laresgoiti-Servitje, E.; Lemus-Martin, R.; Sanchez-Flores, A.; Sanders-Velez, C. The New SARS-CoV-2 Variants and Their Epidemiological Impact in Mexico. *Mbio* **2022**, *13*, e01060-21. [CrossRef] [PubMed]
5. Zhang, Q.; Xiang, R.; Huo, S.; Zhou, Y.; Jiang, S.; Wang, Q.; Yu, F. Molecular mechanism of interaction between SARS-CoV-2 and host cells and interventional therapy. *Signal Transduct. Target. Ther.* **2021**, *6*, 233. [CrossRef] [PubMed]
6. Gorgels, K.M.; Dingemans, J.; van der Veer, B.M.; Hackert, V.; Hensels, A.Y.; den Heijer, C.D.; van Alphen, L.B.; Savelkoul, P.H.M.; Hoebe, C.J. Linked nosocomial COVID-19 outbreak in three facilities for people with intellectual and developmental disabilities due to SARS-CoV-2 variant B. 1.1. 519 with spike mutation T478K in the Netherlands. *BMC Infect. Dis.* **2022**, *22*, 139. [CrossRef] [PubMed]
7. Rodríguez-Maldonado, A.P.; Vázquez-Pérez, J.A.; Cedro-Tanda, A.; Taboada, B.; Boukadida, C.; Wong-Arámbula, C.; Nuñez-García, T.E.; Cruz-Ortiz, N.; Barrera-Badillo, G.; Hernández-Rivas, L.; et al. Emergence and spread of the potential variant of interest (VOI) B. 1.1. 519 of SARS-CoV-2 predominantly present in Mexico. *Arch. Virol.* **2021**, *166*, 3173–3177. [CrossRef] [PubMed]
8. Samson, R.; Navale, G.R.; Dharne, M.S. Biosensors: Frontiers in rapid detection of COVID-19. *3 Biotech* **2020**, *10*, 385. [CrossRef] [PubMed]
9. Soler, M.; Estevez, M.C.; Cardenosa-Rubio, M.; Astua, A.; Lechuga, L.M. How nanophotonic label-free biosensors can contribute to rapid and massive diagnostics of respiratory virus infections: COVID-19 case. *ACS Sens.* **2020**, *5*, 2663–2678. [CrossRef] [PubMed]
10. Lim, J.; Stavins, R.; Kindratenko, V.; Baek, J.; Wang, L.; White, K.; Kumar, J.; Valera, E.; King, W.P.; Bashir, R. Microfluidic point-of-care device for detection of early strains and B. 1.1. 7 variant of SARS-CoV-2 virus. *Lab Chip* **2022**, *22*, 1297–1309. [CrossRef] [PubMed]
11. Ozer, T.; Geiss, B.J.; Henry, C.S. Review Chemical and Biological Sensors for Viral Detection. *J. Electrochem. Soc.* **2020**, *167*, 37523. [CrossRef] [PubMed]
12. Tothill, I.E.; Turner, A.P.F. Biosensors. 2003. Available online: https://www.sciencedirect.com/science/article/pii/B012227055X013742 (accessed on 12 January 2023).
13. El-Sherif, D.M.; Abouzid, M.; Gaballah, M.S.; Ahmed, A.A.; Adeel, M.; Sheta, S.M. New approach in SARS-CoV2 surveillance using biosensor technology: A review. *Environ. Sci. Pollut. Res.* **2022**, *29*, 1677–1695. [CrossRef] [PubMed]
14. Bai, S.; Wang, T.; Zhang, Z.; Sheng, S.; Yu, W.; Xie, G. A novel colorimetric biosensor for detecting target DNA and human alpha thrombin based on associative toehold activation concatemer induced catalyzed hairpin assembly amplification. *Sens. Actuators Chem.* **2017**, *239*, 447–454. [CrossRef]
15. Zhang, L.; Fang, X.; Liu, X.; Ou, H.; Zhang, H.; Wang, J.; Li, Q.; Cheng, H.; Zhang, W.; Luo, Z. Discovery of sandwich type COVID-19 nucleocapsid protein DNA aptamers. *Chem. Commun.* **2020**, *56*, 10235–10238. [CrossRef] [PubMed]
16. Kothandan, R.; Uthayasooriyan, P.; Vairamani, S. Search for RNA aptamers against non-structural protein of SARS-CoV-2: Design using molecular dynamics approach. *Beni-Suef Univ. J. Basic Appl. Sci.* **2021**, *10*, 64. [CrossRef] [PubMed]
17. Poolsup, S.; Zaripov, E.; Hüttmann, N.; Minic, Z.; Artyushenko, P.V.; Shchugoreva, I.A.; Tomilin, F.N.; Kichkailo, A.S.; Berezovski, M.V. Discovery of DNA aptamers targeting SARS-CoV-2 nucleocapsid protein and protein-binding epitopes for label-free COVID-19 diagnostics. *Mol. Ther. Nucleic Acids* **2023**, *31*, 731–743. [CrossRef] [PubMed]
18. Chen, Z.; Wu, Q.; Chen, J.; Ni, X.; Dai, J. A DNA aptamer based method for detection of SARS-CoV-2 nucleocapsid protein. *Virol. Sin.* **2020**, *35*, 351–354. [CrossRef] [PubMed]
19. Ge, C.; Feng, J.; Zhang, J.; Hu, K.; Wang, D.; Zha, L.; Hu, X.; Li, R. Aptamer/antibody sandwich method for digital detection of SARS-CoV2 nucleocapsid protein. *Talanta* **2022**, *236*, 122847. [CrossRef] [PubMed]

20. Li, J.; Sczepanski, J.T. Targeting a conserved structural element from the SARS-CoV-2 genome using l-DNA aptamers. *RSC Chem. Biol.* **2022**, *3*, 79–84. [CrossRef] [PubMed]
21. Zhou, C.; Lin, C.; Hu, Y.; Zan, H.; Xu, X.; Sun, C.; Zou, H.; Li, Y. Sensitive fluorescence biosensor for SARS-CoV-2 nucleocapsid protein detection in cold-chain food products based on DNA circuit and g-CNQDs@ Zn-MOF. *LWT* **2022**, *169*, 114032. [CrossRef] [PubMed]

Disclaimer/Publisher's Note: The statements, opinions and data contained in all publications are solely those of the individual author(s) and contributor(s) and not of MDPI and/or the editor(s). MDPI and/or the editor(s) disclaim responsibility for any injury to people or property resulting from any ideas, methods, instructions or products referred to in the content.